Kinetics and Mechanism of CO Substitution in Six-Coordinate Halotetracarbonylnitrosyltungsten(I)

Yousif Sulfab*,† and Fred Basolo*

Department of Chemistry, Northwestern University, Evanston, Illinois 60208

Arnold L. Rheingold*

Department of Chemistry, University of Delaware, Newark, Delaware 19716

Received December 30, 1988

The substitution of CO in $W(CO)_4(NO)X$ (X = Cl, Br, or I) by PPh_3 proceeds exclusively via a dissociative mechanism. In the reaction with the stronger nucleophile $P(n\text{-}Bu)_3$, both dissociative and associative mechanisms are operative. The enthalpies and entropies of activation associated with k_1 and k_2 support these mechanistic assignments. The monosubstituted complex reacts further with phosphine ligands to form disubstituted products. Formation of the disubstituted complex appears to be dissociative in nature. The X-ray structure of $W(CO)_2(NO)(I)(PMe_2Ph)_2$ is reported: monoclinic, $P2_1/n$, a = 9.729 (2) Å, b = 23.230 (8) Å, c = 10.399 (2) Å, β = 102.86 (2)°, V = 2291.3 (8) Å^3, Z = 4; $R(F)$ = 3.67% for 2841 observed data.

Introduction

Considerable work has been done on the kinetics and mechanisms of CO substitutions in metal carbonyls, but far less is known about reactions of metal nitrosyl carbonyls.[1] Years ago we investigated substitution reactions of the isoelectronic acid isostructural compounds $Ni(CO)_4$,[2] $Co(CO)_3(NO)$,[3] and $Fe(CO)_2(NO)_2$[4] and were surprised to find that $Ni(CO)_4$ reacts by a dissociative process, whereas the nitrosyl carbonyls react primarily by an associative pathway. This difference, prior to the X-ray structure of bent metal nitrosyls[5] and prior to the 16–18-electron rule,[6] was attributed to localizing a pair of electrons on the nitrogen in the transition state in order to vacate a metal orbital for nucleophilic attack (eq 1). The 5-coordinate

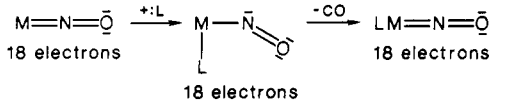

(1)

$Mn(CO)_4(NO)$ also reacts with good nucleophiles by an associative pathway,[7] which too is believed to involve a transition state or intermediate of the type shown in eq 1.

To our knowledge, the only kinetics and mechanism study reported for a 6-coordinate metal nitrosyl carbonyl is for CO substitutions of $V(CO)_5(NO)$.[8] This compound, unlike its isoelectronic and isostructural counterpart $Cr(CO)_6$,[1] is very reactive. One reason is because of the large trans effect of the NO group, which then greatly enhances the rate of dissociation of its trans CO. In addition, good nucleophiles also react by a competing associative pathway, presumably through a bent nitrosyl transition state (eq 1).

There is a need for further studies of CO substitution in 6-coordinate metal nitrosyl carbonyls, particularly systems with no CO trans to NO. This paper reports the results of such a study using *trans*-$W(CO)_4(NO)X$[9] (X = Cl, Br, I). The halo ligands in this system are poor leaving groups, making it possible to study only CO substitution in comparison with earlier results[10b] on the isoelectronic compounds $Re(CO)_5X$ = (X = Cl, Br, I) that are devoid of an NO group.

Experimental Section

Compounds and Solvents. Toluene and pentane were distilled over Na and under N_2. Dichloromethane was distilled under N_2 from P_2O_5. Analytical reagent grade acetonitrile was used without further purification.

Triphenylphosphine (PPh_3) was recrystallized from ethanol and dried over $CaSO_4$. Tri-*n*-butylphosphine ($P(n\text{-}Bu)_3$) and dimethylphenylphosphine (PMe_2Ph) were distilled from sodium under reduced pressure. The tetraalkylammonium salts $(C_2H_5)_4NCl$, $(C_4H_9)_4NBr$, and $(C_4H_9)_4NI$ were dried before use.

The complexes $(C_2H_5)_4N[W(CO)_5Cl]$, $(C_4H_9)_4N[W(CO)_5Br]$, and $(C_4H_9)_4N[W(CO)_5I]$ were prepared according to the published method,[11] and the compounds were characterized by comparing their IR spectra to the spectra of the known compounds.

The halo tetracarbonyl nitrosyl complexes $W(CO)_4(NO)X$ (X = Cl, Br, or I) were prepared by a method analogous to that reported.[9] This involved the slow addition of $NOHSO_4$ to a stirred solution of the tetralkylammonium complex in acetonitrile until the evolution of CO is diminished. In the reactions of the chloro and bromo complexes the nitrosyl complex precipitated from the acetonitrile solution. In a typical experiment to a solution of $(C_4H_9)_4N[W(CO)_5Br]$ (2.3 g, 3.56 mmol) in 10 mL of acetonitrile was slowly added an equivalent amount of $NOHSO_4$ with stirring, and 0.35 g of $[W(CO)_4(NO)Br]$ was obtained (~24%). The iodo complex, which is highly soluble in acetonitrile, was extracted from the solid reaction mixture with 1/1 dichloromethane/pentane after the removal of acetonitrile. All of the complexes were sublimed, and their IR spectra were in excellent agreement with published data.[9]

Product Identification. The monosubstituted complex $W(CO)_3(PPh_3)(NO)Br$ was prepared by reacting $W(CO)_4(NO)Br$ (0.165 g, ~0.40 mmol) with PPh_3 (0.107 g, ~0.40 mmol) in 5 mL

† On leave from the Department of Chemistry, Kuwait University, Kuwait.

(1) Basolo, F. *Inorg. Chim. Acta* **1985**, *100*, 33. Howell, J. A. S.; Burkinshaw, P. M. *Chem. Rev.* **1983**, *83*, 557 and references therin.
(2) Basolo, F.; Wojcicki, A. *J. Am. Chem. Soc.* **1961**, *83*, 5290. Day, J. P.; Pearson, R. G.; Basolo, F. *Ibid.* **1968**, *90*, 6927.
(3) Thorsteinson, E. M.; Basolo, F. *J. Am. Chem. Soc.* **1966**, *88*, 3929.
(4) Morris, D. E.; Basolo, F. *J. Am. Chem. Soc.* **1968**, *90*, 2531, 2536.
(5) Hodgson, D. J.; Ibers, J. A. *Inorg. Chem.* **1969**, *8*, 1282.
(6) Tolman, C. A. *Chem. Soc. Rev.* **1972**, *1*, 337.
(7) Wawarsik, H.; Basolo, F. *J. Am. Chem. Soc.* **1967**, *89*, 4626.
(8) Shi, Q. Z.; Richmond, T. G.; Trogler, W. C.; Basolo, F. *Inorg. Chem.* **1984**, *23*, 957.
(9) Barrclough, C. G.; Bowden, J. A.; Colton, R.; Commons, C. J. *Aust. J. Chem.* **1973**, *26*, 241. Isaacs, E. E.; Graham, W. A. G. *J. Organomet. Chem.* **1975**, *99*, 119. Butler, I. S.; Shaw III, C. F. *J. Raman Spectrosc.* **1975**, *3*, 65.
(10) (a) Angelici, R. J.; Basolo, F. *J. Am. Chem. Soc.* **1962**, *84*, 2495. (b) Brown, D. A.; Sane, R. T. *J. Chem. Soc. A* **1971**, 2088.
(11) Abel, E. W.; Butler, I. S.; Reid, I. G. *J. Chem. Soc.* **1963**, 2068.

0276-7333/89/2308-2139$01.50/0

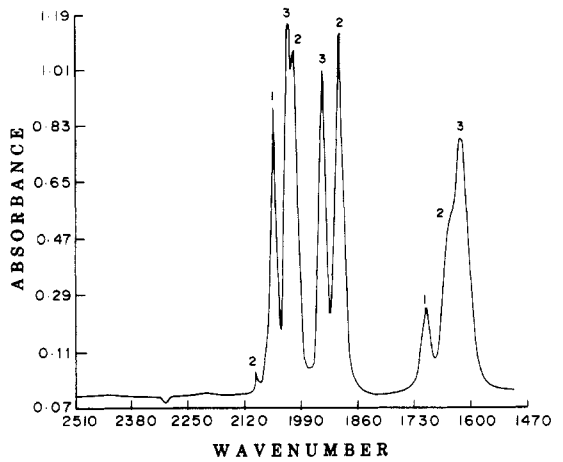

Figure 1. IR absorbance spectra of a solution containing 2:1 $[P(n\text{-}Bu)_3]$:$[W(CO)_4(NO)Br]$ in dichloromethane at equilibrium at room temperature. The parent complex ν_{CO} appears at 2051 cm^{-1} (1). The ν_{CO} of the monosubstituted complex $W(CO)_3(NO)P(n\text{-}Bu)_3Br$ appear at ~2093, 2004, and 1900 cm^{-1} (2). The ν_{CO} of the disubstituted complex appears at 2018 and 1939 cm^{-1} (3). The ν_{NO} for the parent, the monosubstituted, and disubstituted complexes are shown at 1701 (1), 1647 (2), and 1619 cm^{-1} (3), respectively.

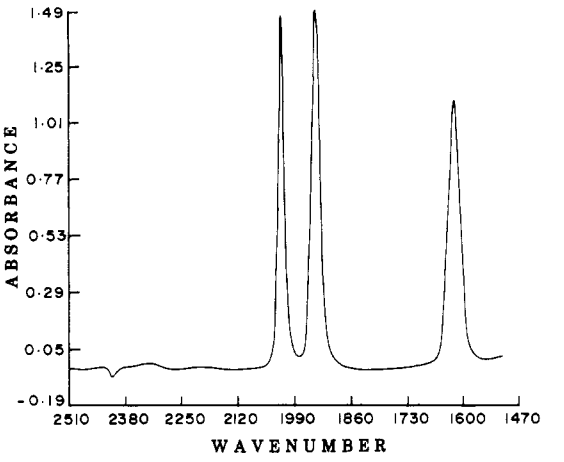

Figure 2. IR absorbance spectrum of the disubstituted complex $W(CO)_2(NO))(P(n\text{-}Bu)_3)_2Br$. The ν_{CO} appears at 2018 and 1939 cm^{-1} and the ν_{NO} at 1621 cm^{-1}.[2]

of dichloromethane at room temperature. After the ν_{CO} of the parent complex had disappeared, the product was precipitated by the addition of pentane. The solvents were removed, and the yellow solid was recrystallized from a dichloromethane/pentane solution. Anal. Calcd for $W(CO)_3(PPh_3)(NO)Br$: C, 39.40; H, 2.36; N, 2.19. Found: C, 38.80; H, 2.31; N, 2.19. MS: *m/e* (relative intensity) $(MH)^+$ 641 (14.65), $(MH - CO)^+$ 613 (16.4), $(MH - 2CO)^+$ 585 (100), $(MH - 3CO)^+$ 557 (75.9).

The reactions of the $W(CO)_4(NO)X$ complexes with excess phosphine ligands afford the formation of the disubstituted product. Even with only a 1:1 mole ratio of substrte and phosphine, a noticeable amount of the disubstituted product is formed. In Figure 1 the monosubstituted product $W(CO)_3(NO)P(n\text{-}Bu)_3Br$ has three ν_{CO} at 2093, 2004, and 1900 cm^{-1} and ν_{NO} at 1650 cm^{-1}. The disubstituted product $W(CO)_2(NO)(P(n\text{-}Bu)_3)_2Br$ has two ν_{CO} at 2018 and 1940 cm^{-1}, and the ν_{NO} is lowered to 1621 cm^{-1}. The mono- and disubstituted products of the reaction of the bromo complex with PPh_3 showed similar IR behavior.

Disubstituted products were isolated employing PMe_2Ph using the bromo and iodo complexes. To a solution of ~0.2 mmol of the complex in 4 mL of dichloromethane was added a tenfold excess of PMe_2Ph, and the reaction mixture was stirred at room temperature. After the disappearance of the CO and NO IR bands of the parent and the monosubstituted complexes, pentane was added to the reaction mixture which was then placed in a refrigerator. The crystals that settled were collected on filter paper and air-dried. Anal. Calcd for $W(CO)_2(PMe_2Ph)_2(NO)Br$: C, 34.52; H, 3.54; N, 2.24. Found: C, 34.18; H, 3.37; N, 2.35. MS: *m/e* (relative intensity) MH^+ 628 (12.5), $(MH - CO)^+$ 600 (31.6), $(MH - 2CO)^+$ 572 (100). Anal. Calcd for $W(CO)_2(PMe_2Ph)_2(NO)I$: C, 32.10; H, 3.29; N, 2.08. Found: C, 32.43; H, 3.21; N, 2.18.

Kinetic Measurements. Solutions of the complex and the phosphine ligand, each in toluene, were thermally equilibrated before they were thoroughly mixed, and the reaction solution was kept in a constant temperature bath (±0.1 °C). At different time intervals depending on the reaction rate, aliquots were removed and the absorbance changes in the carbonyl stretching frequency were measured on a Nicolet 7199 FT-IR spectrophotometer. Rates of formation of the monosubstituted product were followed by measuring the disappearance of the carbonyl absorbance. Plots of $-\ln A_t$ vs time were linear over 2–3 half-lives (linear correlation coefficient > 0.990). The rate constant k_{obs} was obtained from the slopes of the linear plots. Pseudo-first-order conditions were maintained in all runs by using at least a tenfold excess of the phosphine ligand concentration. A limited number of kinetic runs were performed where the rate of formation of the disubstituted complex was measured. In these instances k_{obs} was obtained from plots of $\ln (A_\infty - A_t)$ vs time where A_t and A_∞ are absorbances at time t and at infinite reaction time, respectively.

Crystal Structure Determination. Crystals of $[(PMe_2Ph)_2W(NO)(CO)_2I]$ were mounted on glass fibers. Photographic characterization revealed $2/m$ Laue symmetry, and systematic absences uniquely defined the space group as $P2_1/n$. A semiempirical correction for absorption (ψ scan method, six reflections, 216 data) and one for a 12% linear decay in intensity were applied to the data.

The W and I atoms were obtained by direct methods. The location of the NO ligand was distinguished from the CO ligands by conspicuous discrepancies in the thermal parameters for the N and C atoms when incorrectly assigned; the reported assignment shows an agreement in the isotropic equivalent thermal parameters for the ipso atoms of these three ligands that is within the parameters' estimated standard deviations. The phenyl rings were constrained to rigid hexagonal bodies (d(C–C) = 1.395 Å). All non-hydrogen atoms were anisotropically refined, and all hydrogen atoms were idealized (d(C–H) = 0.96 Å).

All computations used SHELXTL (5.1) software (G. Sheldrick, Nicolet XRD, Madison, WI).

Results

The reactions of $W(CO)_4(NO)X$ (X = Cl, Br, I) with PPh_3 and with $P(n\text{-}Bu)_3$ give initially the monosubstituted product but finally produce the disubstituted complexes, as shown in Figures 1 and 2, respectively (eq 2 and 3).

$$W(CO)_4(NO)X + L \rightarrow W(CO)_3(NO)LX + CO \quad (2)$$

$$X = Cl, Br, I; L = PPh_3, P(n\text{-}Bu)_3$$

$$W(CO)_3(NO)LX + L \rightarrow W(CO)_2(NO)L_2X + CO \quad (3)$$

The results in Table I show that the rate of reaction of the parent complex is independent of the PPh_3 concentration, and the rate law is described by eq 4. The values of k_1 calculated at various temperatures are collected in Table I.

$$-\frac{d[W(CO)_4(NO)X]}{dt} = k_1[W(CO)_4(NO)X] \quad (4)$$

The kinetics of CO substitution by $P(n\text{-}Bu)_3$ in $(W(CO)_4(NO)X)$ proceeds in two stages where the relatively faster formation of a monosubstituted product is followed by a slower generation of a disubstituted product (Figures 1 and 2). A similar reaction occurs with PMe_2Ph instead of $P(n\text{-}Bu)_3$, where the formation of the disubstituted product was confirmed by isolating the crystalline product $W(CO)_2(PMe_2Ph)_2(NO)I$ from a solution containing an excess of PMe_2Ph. The IR spectrum of these crystals is identical with that shown in Figure 2 for the solution reaction disubstituted product. Elemental analyses and

Table I. Kinetic Data for the Substitution of CO by PPh_3 in $[W(CO)_4(NO)X]$ in Toluene

X	T, °C	$[PPh_3]$, M	10^4k_1, s^{-1}	ΔH_1^*, kcal mol^{-1}	ΔS_1^*, cal deg^{-1} mol^{-1}
Cl	30.0	0.050	5.49 ± 0.14	27.8 ± 2.4[a]	18.4 ± 2.2[a]
	25.0	0.050	2.79 ± 0.08	(27.3)[b]	(6.2)[b]
		0.300	2.83 ± 0.10		
	20.0	0.050	0.96 ± 0.02		
		0.300	0.98 ± 0.04		
Br	40.0	0.050	4.57 ± 0.01	28.1 ± 0.1[c]	15.8 ± 0.9[c]
	35.0	0.050	2.33 ± 0.06	(29.3)[b]	(9.8)[b]
		0.100	2.31 ± 0.02		
		0.200	2.31 ± 0.03		
		0.300	2.36 ± 0.04		
	30.0	0.050	1.17 ± 0.06		
I	45.0	0.050	2.29 ± 0.03	30.7 ± 1.3	21.3 ± 1.3
	40.0	0.050	1.10 ± 0.02	(31.8)[b]	(12.9)[b]
	35.0	0.050	0.46 ± 0.01		
		0.300	0.42 ± 0.01		

[a] Values of ΔH^* and ΔS^* were calculated by using also the k_1 intercept values from data in Table II of 2.87×10^{-4} at 25 °C and of 1.10×10^{-4} at 20 °C. [b] Values in parentheses are for the same reactions of the corresponding isoelectronic compounds $Re(CO)_5X$. [c] Values of ΔH^* and ΔS^* were calculated by using also the k_1 intercept values from data in Table II of 2.21×10^{-4} at 35 °C and of 1.00×10^{-4} at 30 °C.

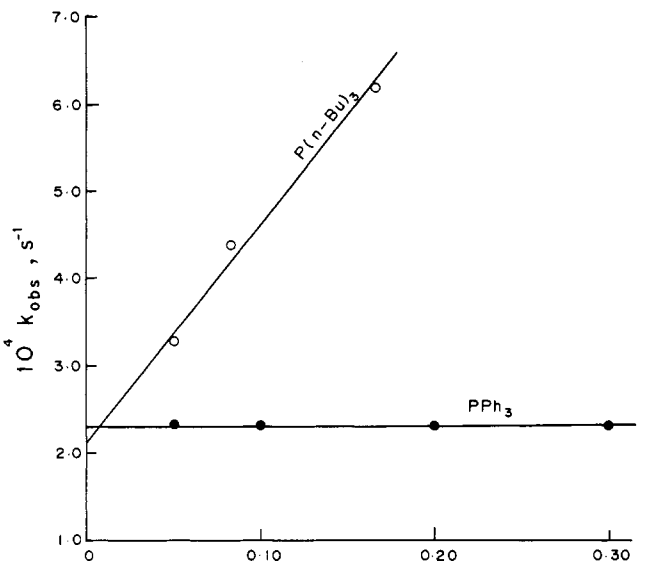

Figure 3. Plots of k_{obs} vs $[PR_3]$ for the reaction of $W(CO)_3(NO)P(n\text{-}Bu)_3Br$ in toluene at 35 °C to form the monosubstituted product.

X-ray structure confirm the complex is the disubstituted product.

The results in Table II show that the rate of formation of the monosubstituted product with $P(n\text{-}Bu)_3$ is dependent on the concentration of phosphine. Plots of k_{obs} vs $[P(n\text{-}Bu)_3]$ at various temperatures for the bromo complex are shown in Figure 3. These plots are consistent with the two-term rate law of eq 5. Similar plots were also

$$-\frac{d[W(CO)_4(NO)X]}{dt} = (k_1 + k_2[P(n\text{-}Bu)_3])[W(CO)_4(NO)X] \quad (5)$$

found for the chloro and the iodo complexes. The values of k_1 and k_2 obtained from the intercepts and the slopes, respectively, of the plots of k_{obs} vs $[P(n\text{-}Bu)_3]$ are given in Table II.

The kinetics of formation of the disubstituted complex has not been investigated in great detail. The limited results in Table III show that its rate of formation is not greatly affected by the concentration of phosphine ligand.

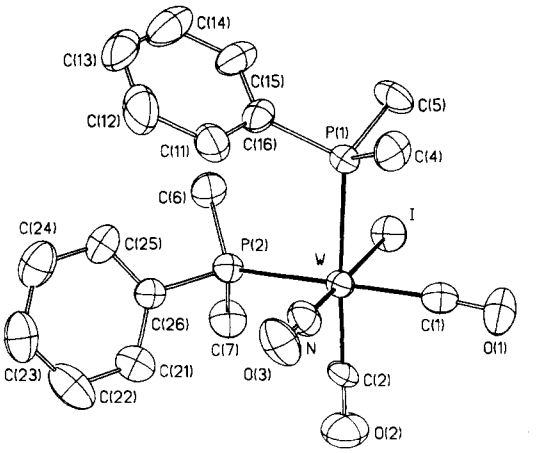

Figure 4. Molecular structure of $[(PhMe_2)_2W(NO)(CO)_2I]$ with 40% thermal ellipsoids.

Scheme I

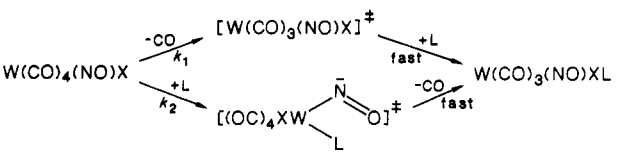

The enthalpies and entropies of activation associated with the ligand-independent pathway (ΔH_1^* and ΔS_1^*) and with the ligand-dependent process (ΔH_2^* and ΔS_2^*) are shown in Tables I and II, respectively. The enthalpy (ΔH^*) and entropy (ΔS^*) of formation of the disubstituted product are reported in Table III. Crystallographic data are collected in Table IV. The atomic coordinates are given in Table V, and selected bond distances and angles in Table VI. The ORTEP drawing is shown in Figure 4.

Discussion

Substitution of the first CO in $W(CO)_4(NO)X$ by the poor nucleophile PPh_3 proceeds via a dissociative mechanism within the limits of our experiments. This is indicated by the independence of the rate of these reactions on the concentration of the PPh_3 ligand (Table I and Figure 3). Data in Table I also show that the rate of reaction of $W(CO)_4(NO)X$ decreases with changes in X in the order Cl > Br > I. This same order was observed[10] for the isoelectronic $Re(CO)_5X$ compounds and the $Mn(CO)_5X$ compounds. The rates of dissociation of the nitrosyl complexes $W(CO)_4(NO)X$ are about 2 orders of magnitude faster than for the corresponding $Re(CO)_5X$ compounds. However, for each compound the difference in rates between the different halogen compounds are about the same. This decrease in reactivity with increase in atomic number of the halogen was attributed[10] to a decrease in polarizability (or electronegativity) of the X ligand. Such a decrease in electronegativity of X allows more electron density on the metal for π back-bonding to CO, thus increasing the M–CO bond strength and decreasing the rate of dissociation. The carbonyl frequencies of $W(CO)_4(NO)X$ reflect this trend, with values of ν_{CO} being 2049, 2048, and 2045 cm^{-1} in toluene for the chloro, bromo, and iodo complexes, respectively.

The good nucleophile $P(n\text{-}Bu)_3$ reacts with $W(CO)_4(NO)X$ (eq 2) more rapidly than does PPh_3, and the reaction involves a two-term rate law (eq 5). This suggests parallel dissociative (k_1) and associative (k_2) pathways, in accordance with Scheme I. Scheme I is supported by the observation that a plot of k_{obs} vs $P(n\text{-}Bu)_3$ gives extrapo-

Table II. Kinetic Data for the Substitution of CO by P(*n*-Bu)$_3$ in [W(CO)$_4$(NO)X] in Toluene

X	*T*, °C	[P(*n*-Bu)$_3$], M	10^4k_{obs}, s^{-1}	10^4k_1, s^{-1}	10^3k_2, M^{-1} s^{-1}	$\Delta H_2^{\ddagger}$, kcal mol^{-1}	$\Delta S_2^{\ddagger}$, cal deg^{-1} mol^{-1}
Cl	25.0	0.050	3.75 ± 0.13	2.87 ± 0.05	1.80 ± 0.04	9.6 ± 1.8	−39.0 ± 28.2
		0.100	4.70 ± 0.20				
		0.180	6.10 ± 0.12				
	20.0	0.050	1.90 ± 0.05	1.10 ± 0.10	1.47 ± 0.10		
		0.150	3.17 ± 0.16				
		0.270	5.12 ± 0.24				
	15.0	0.100	1.18 ± 0.10	0.28 ± 0.37	0.995 ± 0.170		
		0.200	2.47 ± 0.07				
		0.300	3.17 ± 0.10				
Br	35.0	0.050	3.28 ± 0.01	2.21 ± 0.29	2.39 ± 0.26	15.3 ± 2.6	−20.8 ± 6.7
		0.083	4.37 ± 0.10				
		0.167	6.15 ± 0.27				
	30.0	0.050	1.86 ± 0.05	1.00 ± 0.04	1.76 ± 0.02		
		0.083	2.51 ± 0.04				
		0.167	3.93 ± 0.06				
		0.250	5.42 ± 0.17				
	25.0	0.108	1.41 ± 0.04	0.30 ± 0.13	1.00 ± 0.05		
		0.167	1.91 ± 0.03				
		0.250	2.82 ± 0.05				
I	45.4	0.050	3.22 ± 0.10	2.44 ± 0.01	1.57 ± 0.01	16.3 ± 0.2	−20.3 ± 0.5
		0.120	4.32 ± 0.19				
		0.200	5.57 ± 0.13				
	40.0	0.050	1.63 ± 0.04	1.08 ± 0.12	0.995 ± 0.060		
		0.150	2.48 ± 0.06				
		0.300	4.10 ± 0.05				
	35.0	0.050	0.79 ± 0.01	0.49 ± 0.04	0.637 ± 0.022		
		0.150	1.48 ± 0.01				
		0.300	2.39 ± 0.05				

Table III. Rate Constants for CO Substitution by P(*n*-Bu)$_3$ in W(CO)$_3$(NO)P(*n*-Bu)$_3$Br in Toluene

X	*T*, °C	[(*n*-Bu)$_3$P], M	10^4k_1, s^{-1}	$\Delta H_1^{\ddagger}$, kcal mol^{-1}	$\Delta S_1^{\ddagger}$, cal deg^{-1} mol^{-1}
Cl	30.5	0.050	1.08		
		0.150	0.95		
	35.0	0.100	1.54		
Br	30.0	0.250	0.48	40.8 ± 4.6	56.2 ± 8.0
	35.0	0.250	1.19		
	40.0	0.250	4.38		

Table IV. Crystallography Parameters for [(PPhMe$_2$)$_2$W(CO)$_2$(NO)I]

(a) Crystal Data

formula	$C_{18}H_{22}INP_2O_3W$	*V*, Å^3	2291.3 (8)
cryst system	monoclinic	*Z*	4
space group	$P2_1/n$	*D*(calcd), g cm^{-3}	1.951
a,[a] Å	9.729 (2)	μ(Mo Kα), cm^{-1}	68.1
b, Å	23.230 (8)	temp, K	292
c, Å	10.399 (2)	color	orange
β, deg	102.86 (2)	size, mm	0.28 × 0.31 × 0.32

(b) Data Collection

diffractometer	Nicolet R3m/μ	reflns colltd	4215
radiation	Mo Kα	indpdt reflns	3911
λ, Å	0.71073	obs rflns (5 $\sigma(F_o)$)	2841
monochromator	graphite	*R*(int), %	7.1
scan limits, deg	$4 \le 2\theta \le 50$	decay, %	12
octants collctd	$\pm h,+k,+l$	*T*(max)/*T*(min)	3.3
scan method	Wyckoff		

(c) Refinement

R(*F*), %	3.67	Δ/σ(final)	0.030
R(*wF*), %	4.01	$\Delta(P)$, e Å^{-3}	1.47
GOF	1.062	N_o/N_v	13.5

[a] Unit cell parameters from the best fit of the angular settings of 25 reflections ($26° \le 2\theta \le 30°$).

lated values of k_1 in good agreement with the k_1 values for reaction with PPh_3 (Figure 3 and Tables I and II). Similar reaction processes were proposed earlier[3,4,7] for CO substitution reactions of metal nitrosyl carbonyls with metals

Table V. Atomic Coordinates (×10^4) and Isotropic Thermal Parameters (Å^2 × 10^3) for [(PhMe$_2$)$_2$W(NO)(CO)$_2$I]

	x	*y*	*z*	*U*[a]
W	7478.3 (4)	1568.0 (2)	−826.7 (3)	48.0 (1)
I	8155.6 (9)	643.6 (3)	997.0 (7)	80.7 (3)
P(1)	9996 (2)	1544 (1)	−1245 (2)	49 (1)
P(2)	6485 (3)	770 (1)	−2459 (2)	56 (1)
O(3)	6900 (8)	2569 (3)	−2779 (7)	88 (3)
O(2)	4529 (9)	1743 (4)	−256 (10)	117 (4)
O(1)	8507 (8)	2404 (3)	1578 (7)	95 (3)
C(1)	8197 (9)	2105 (4)	681 (9)	61 (4)
N	7108 (8)	2174 (3)	−2043 (7)	65 (3)
C(2)	5672 (9)	1654 (4)	−466 (9)	60 (4)
C(4)	10806 (10)	2248 (4)	−1105 (9)	71 (4)
C(5)	11282 (10)	1123 (4)	−98 (9)	77 (4)
C(6)	7606 (12)	174 (4)	−2666 (10)	83 (5)
C(7)	5050 (11)	401 (5)	−1946 (10)	89 (5)
C(11)	9620 (7)	1685 (3)	−3943 (7)	86 (5)
C(12)	9737	1529	−5209	131 (8)
C(13)	10417	1018	−5404	139 (9)
C(14)	10982	664	−4333	113 (7)
C(15)	10865	820	−3067	80 (5)
C(16)	10184	1331	−2871	61 (3)
C(21)	4398 (6)	1270 (3)	−4396 (7)	79 (5)
C(22)	3775	1441	−5678	98 (6)
C(23)	4467	1344	−6698	95 (6)
C(24)	5781	1074	−6435	95 (6)
C(25)	6404	903	−5152	80 (5)
C(26)	5712	1000	−4133	51 (3)

[a] Equivalent isotropic *U* defined as one-third of the trace of the orthogonalized U_{ij} tensor.

of coordination number lower than six. This is the second report of CO substitution of a 6-coordinate metal nitrosyl carbonyl via a 7-coordinate transition state or intermediate, the first being the reaction of $V(CO)_5NO$.[8] Here there is plenty of precedence[12] for stable 7-coordinate tungsten complexes, supporting the suggestion of an associative process with an expansion of the coordination number of tungsten. Furthermore, although no direct evidence is available for the presumed 18-electron, 7-coordinate

(12) King, R. B. *Inorg. Chem.* **1964**, *3*, 1039 and references therein.

Table VI. Selected Bond Distances and Angles for $[(PhMe_2P)_2WI(CO)_2(NO)]$

(a) Bond Distances (Å)			
W-I	2.844 (1)	W-N	1.873 (8)
W-P(1)	2.582 (2)	C(1)-O(1)	1.149 (11)
W-P(2)	2.554 (2)	C(2)-O(2)	1.198 (13)
W-C(1)	2.003 (9)	N-O(3)	1.184 (10)
W-C(2)	1.887 (9)		
(b) Bond Angles (deg)			
I-W-P(1)	90.5 (1)	P(2)-W-C(1)	170.6 (3)
I-W-P(2)	83.8 (1)	P(2)-W-C(2)	88.7 (3)
I-W-C(1)	87.7 (3)	P(2)-W-N	96.2 (2)
I-W-C(2)	92.0 (3)	C(1)-W-C(2)	87.5 (4)
I-W-N	177.6 (2)	C(1)-W-N	92.4 (3)
P(1)-W-P(2)	96.0 (1)	C(2)-W-N	90.4 (4)
P(1)-W-C(1)	88.1 (3)	W-N-O(3)	177.7 (7)
P(1)-W-C(2)	174.8 (3)	W-C(1)-O(1)	174.4 (9)
P(1)-W-N	87.1 (2)	w-C(2)-O(2)	176.1 (8)

transition state, there is ample reason to believe that the associative pathway does not involve a high energy 20-electron system. For example, no such pathway is available to the isoelectronic $Re(CO)_5X$ compounds.

The reactivity of the $[W(CO)_4(NO)X]$ complexes by either the dissociative or the associative path is less than that of the 6-coordinate $V(CO)_5NO$.[8] However, the value of k_2 is comparable to those of $Co(CO)_3NO$[3] and $Fe(CO)_2(NO)_2$.[4] The higher reactivity of $V(CO)_5NO$ has been attributed to the trans effect of the NO ligand.

The enthalpy (ΔH_1^*) and entropy (ΔS_1^*) of activation associated with the k_1 path are consistent with a dissociative mechanism. A dissociative process is usually characterized by a large enthalpy and positive entropy of activation. Using the kinetic data obtained for the reaction of $W(CO)_4NOBr$ with PPh_3, a ΔH_1^* value of 25.1 kcal mol^{-1} is obtained which seems spuriously low relative to the values of the other two halo complexes. Calculations made also by using intercept values of k_1 for reactions with $P(n\text{-}Bu)_3$ give $\Delta H^* = 28.1$ kcal mol^{-1} (see Table I) which appears to be a more reliable value. For the ligand-dependent pathway, low values of ΔH_2^* and negative values of ΔS_2^* (Table II) support an associative mechanism.

The independence of the k_1 term on ligand concentration for the formation of the disubstituted product coupled with the high value of ΔH_1^* and the positive ΔS_1^* value supports a dissociative mechanism. The high value of ΔH_1^* for this process is expected, since removal of a second CO is more difficult due to the higher electron density on tungsten resulting in greater π back-bonding and stronger W-CO bonds.

At one point in our study, we believed there was spectroscopic evidence for the intermediate formation of the bent nitrosyl $W(CO)_4(NO)IP(n\text{-}Bu)_3$. It was possible to obtain suitable crystals of what was believed to be the corresponding PMe_2Ph compound, but elemental analyses and X-ray structure showed it to be the disubstituted compound $W(CO)_2(NO)(I)(PMe_2Ph)_2$. The ORTEP drawing

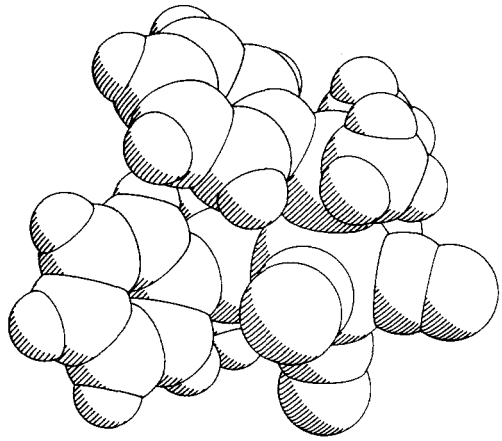

Figure 5. A space-filling drawing of $[(PhMe_2)_2W(NO)(CO)_2I]$ in approximately the same orientation as Figure 4. This view reveals the different CO ligand environments created by their relationship to the phosphine methyl groups (see text).

of this compound is shown in Figure 4, and crystallographic information is given in Tables IV, V, and VI. There is reason to feel quite certain about the NO vs CO ligand assignment despite the significant differences in the W–C distances; W–C(1) is 2.003 and W–C(2) is 1.887 (9) Å. By comparison to other W carbonyls, the W–C(2) distance is short, the other normal. Although the two CO environments appear chemically idential (both trans to PMe_2Ph), their relationships to the phosphine methyl groups differ considerably. The substituents of the P(1) phosphine make more close intramolecular contacts than do those of P(2). This leads to an elongation of the W–P(1) bond. In turn, by a trans-effect process the W–C(2) distance shortens. The C–O distances agree; i.e., C(1)–O(1) is shorter than C(2)–O(2). This is made clearer by the space-filling drawing (Figure 5) of $W(CO)_2(NO)I(PMe_2Ph)_2$ in approximately the same orientation as the ORTEP (Figure 4). This view reveals the different CO ligand environments created by their relationship to the phosphine methyl groups.

Acknowledgment. This research was supported by the National Science Foundation under Grant No. CHE-8514366 and by a Presidential Grant from Northwestern University. We also thank Kuwait University for awarding Y.S. a year's leave of absence to do this research.

Registry No. $W(CO)_4(NO)Cl$, 39899-80-4; $W(CO)_4(NO)Br$, 39899-81-5; $W(CO)_4(NO)I$, 39899-82-6; PPh_3, 603-35-0; $P(n\text{-}Bu)_3$, 998-40-3; $W(CO)_3(NO)P(n\text{-}Bu)_3Cl$, 121788-85-0; $W(CO)_3(NO)P(n\text{-}Bu)_3Br$, 121788-86-1; $(PPhMe_2)_2W(CO)_2(NO)I$, 42593-51-1.

Supplementary Material Available: Tables of isotropic thermal parameters, complete bond lengths and angles, and calculated hydrogen atom positions (4 pages); a listing of structure factors (23 pages). Ordering information is given on any current masthead page.